# Evidence for the $h_b(1P)$ meson in the decay $\Upsilon(3S) \to \pi^0 h_b(1P)$

J. P. Lees,[1] V. Poireau,[1] E. Prencipe,[1] V. Tisserand,[1] J. Garra Tico,[2] E. Grauges,[2] M. Martinelli[ab,3]

D. A. Milanes[ab,3] A. Palano[ab,3] M. Pappagallo[ab,3] G. Eigen,[4] B. Stugu,[4] L. Sun,[4] D. N. Brown,[5] L. T. Kerth,[5]

Yu. G. Kolomensky,[5] G. Lynch,[5] I. L. Osipenkov,[5] H. Koch,[6] T. Schroeder,[6] D. J. Asgeirsson,[7] C. Hearty,[7]

T. S. Mattison,[7] J. A. McKenna,[7] A. Khan,[8] V. E. Blinov,[9] A. R. Buzykaev,[9] V. P. Druzhinin,[9] V. B. Golubev,[9]

E. A. Kravchenko,[9] A. P. Onuchin,[9] S. I. Serednyakov,[9] Yu. I. Skovpen,[9] E. P. Solodov,[9] K. Yu. Todyshev,[9]

A. N. Yushkov,[9] M. Bondioli,[10] S. Curry,[10] D. Kirkby,[10] A. J. Lankford,[10] M. Mandelkern,[10] D. P. Stoker,[10]

H. Atmacan,[11] J. W. Gary,[11] F. Liu,[11] O. Long,[11] G. M. Vitug,[11] C. Campagnari,[12] T. M. Hong,[12] D. Kovalskyi,[12]

J. D. Richman,[12] C. A. West,[12] A. M. Eisner,[13] J. Kroseberg,[13] W. S. Lockman,[13] A. J. Martinez,[13] T. Schalk,[13]

B. A. Schumm,[13] A. Seiden,[13] C. H. Cheng,[14] D. A. Doll,[14] B. Echenard,[14] K. T. Flood,[14] D. G. Hitlin,[14]

P. Ongmongkolkul,[14] F. C. Porter,[14] A. Y. Rakitin,[14] R. Andreassen,[15] M. S. Dubrovin,[15] B. T. Meadows,[15]

M. D. Sokoloff,[15] P. C. Bloom,[16] W. T. Ford,[16] A. Gaz,[16] M. Nagel,[16] U. Nauenberg,[16] J. G. Smith,[16]

S. R. Wagner,[16] R. Ayad,[17, *] W. H. Toki,[17] H. Jasper,[18] A. Petzold,[18] B. Spaan,[18] M. J. Kobel,[19] K. R. Schubert,[19]

R. Schwierz,[19] D. Bernard,[20] M. Verderi,[20] P. J. Clark,[21] S. Playfer,[21] J. E. Watson,[21] D. Bettoni[a,22] C. Bozzi[a,22]

R. Calabrese[ab,22] G. Cibinetto[ab,22] E. Fioravanti[ab,22] I. Garzia[ab,22] E. Luppi[ab,22] M. Munerato[ab,22] M. Negrini[ab,22]

L. Piemontese[a,22] R. Baldini-Ferroli,[23] A. Calcaterra,[23] R. de Sangro,[23] G. Finocchiaro,[23] M. Nicolaci,[23]

S. Pacetti,[23] P. Patteri,[23] I. M. Peruzzi,[23, †] M. Piccolo,[23] M. Rama,[23] A. Zallo,[23] R. Contri[ab,24] E. Guido[ab,24]

M. Lo Vetere[ab,24] M. R. Monge[ab,24] S. Passaggio[a,24] C. Patrignani[ab,24] E. Robutti[a,24] B. Bhuyan,[25] V. Prasad,[25]

C. L. Lee,[26] M. Morii,[26] A. J. Edwards,[27] A. Adametz,[28] J. Marks,[28] U. Uwer,[28] F. U. Bernlochner,[29] M. Ebert,[29]

H. M. Lacker,[29] T. Lueck,[29] P. D. Dauncey,[30] M. Tibbetts,[30] P. K. Behera,[31] U. Mallik,[31] C. Chen,[32] J. Cochran,[32]

H. B. Crawley,[32] W. T. Meyer,[32] S. Prell,[32] E. I. Rosenberg,[32] A. E. Rubin,[32] A. V. Gritsan,[33] Z. J. Guo,[33]

N. Arnaud,[34] M. Davier,[34] D. Derkach,[34] J. Firmino da Costa,[34] G. Grosdidier,[34] F. Le Diberder,[34] A. M. Lutz,[34]

B. Malaescu,[34] A. Perez,[34] P. Roudeau,[34] M. H. Schune,[34] A. Stocchi,[34] L. Wang,[34] G. Wormser,[34] D. J. Lange,[35]

D. M. Wright,[35] I. Bingham,[36] C. A. Chavez,[36] J. P. Coleman,[36] J. R. Fry,[36] E. Gabathuler,[36] D. E. Hutchcroft,[36]

D. J. Payne,[36] C. Touramanis,[36] A. J. Bevan,[37] F. Di Lodovico,[37] R. Sacco,[37] M. Sigamani,[37] G. Cowan,[38]

S. Paramesvaran,[38] A. C. Wren,[38] D. N. Brown,[39] C. L. Davis,[39] A. G. Denig,[40] M. Fritsch,[40] W. Gradl,[40]

A. Hafner,[40] K. E. Alwyn,[41] D. Bailey,[41] R. J. Barlow,[41] G. Jackson,[41] G. D. Lafferty,[41] R. Cenci,[42] B. Hamilton,[42]

A. Jawahery,[42] D. A. Roberts,[42] G. Simi,[42] C. Dallapiccola,[43] E. Salvati,[43] R. Cowan,[44] D. Dujmic,[44] G. Sciolla,[44]

D. Lindemann,[45] P. M. Patel,[45] S. H. Robertson,[45] M. Schram,[45] P. Biassoni[ab,46] A. Lazzaro[ab,46] V. Lombardo[a,46]

F. Palombo[ab,46] S. Stracka[ab,46] L. Cremaldi,[47] R. Godang,[47, ‡] R. Kroeger,[47] P. Sonnek,[47] D. J. Summers,[47]

X. Nguyen,[48] P. Taras,[48] G. De Nardo[ab,49] D. Monorchio[ab,49] G. Onorato[ab,49] C. Sciacca[ab,49] G. Raven,[50]

H. L. Snoek,[50] C. P. Jessop,[51] K. J. Knoepfel,[51] J. M. LoSecco,[51] W. F. Wang,[51] L. A. Corwin,[52] K. Honscheid,[52]

R. Kass,[52] N. L. Blount,[53] J. Brau,[53] R. Frey,[53] J. A. Kolb,[53] R. Rahmat,[53] N. B. Sinev,[53] D. Strom,[53]

J. Strube,[53] E. Torrence,[53] G. Castelli[ab,54] E. Feltresi[ab,54] N. Gagliardi[ab,54] M. Margoni[ab,54] M. Morandin[a,54]

M. Posocco[a,54] M. Rotondo[a,54] F. Simonetto[ab,54] R. Stroili[ab,54] E. Ben-Haim,[55] M. Bomben,[55] G. R. Bonneaud,[55]

H. Briand,[55] G. Calderini,[55] J. Chauveau,[55] O. Hamon,[55] Ph. Leruste,[55] G. Marchiori,[55] J. Ocariz,[55] S. Sitt,[55]

M. Biasini[ab,56] E. Manoni[ab,56] A. Rossi[ab,56] C. Angelini[ab,57] G. Batignani[ab,57] S. Bettarini[ab,57] M. Carpinelli[ab,57, §]

G. Casarosa[ab,57] A. Cervelli[ab,57] F. Forti[ab,57] M. A. Giorgi[ab,57] A. Lusiani[ac,57] N. Neri[ab,57] E. Paoloni[ab,57]

G. Rizzo[ab,57] J. J. Walsh[a,57] D. Lopes Pegna,[58] C. Lu,[58] J. Olsen,[58] A. J. S. Smith,[58] A. V. Telnov,[58] F. Anulli[a,59]

G. Cavoto[a,59] R. Faccini[ab,59] F. Ferrarotto[a,59] F. Ferroni[ab,59] M. Gaspero[ab,59] L. Li Gioi[a,59] M. A. Mazzoni[a,59]

G. Piredda[a,59] C. Bünger,[60] T. Hartmann,[60] T. Leddig,[60] H. Schröder,[60] R. Waldi,[60] T. Adye,[61] E. O. Olaiya,[61]

F. F. Wilson,[61] S. Emery,[62] G. Hamel de Monchenault,[62] G. Vasseur,[62] Ch. Yèche,[62] M. T. Allen,[63] D. Aston,[63]

D. J. Bard,[63] R. Bartoldus,[63] J. F. Benitez,[63] C. Cartaro,[63] M. R. Convery,[63] J. Dorfan,[63] G. P. Dubois-Felsmann,[63]

W. Dunwoodie,[63] R. C. Field,[63] M. Franco Sevilla,[63] B. G. Fulsom,[63] A. M. Gabareen,[63] M. T. Graham,[63]

P. Grenier,[63] C. Hast,[63] W. R. Innes,[63] M. H. Kelsey,[63] H. Kim,[63] P. Kim,[63] M. L. Kocian,[63] D. W. G. S. Leith,[63]

P. Lewis,[63] S. Li,[63] B. Lindquist,[63] S. Luitz,[63] V. Luth,[63] H. L. Lynch,[63] D. B. MacFarlane,[63] D. R. Muller,[63]
H. Neal,[63] S. Nelson,[63] C. P. O'Grady,[63] I. Ofte,[63] M. Perl,[63] T. Pulliam,[63] B. N. Ratcliff,[63] S. H. Robertson,[63]
A. Roodman,[63] A. A. Salnikov,[63] V. Santoro,[63] R. H. Schindler,[63] J. Schwiening,[63] A. Snyder,[63] D. Su,[63]
M. K. Sullivan,[63] S. Sun,[63] K. Suzuki,[63] J. M. Thompson,[63] J. Va'vra,[63] A. P. Wagner,[63] M. Weaver,[63]
W. J. Wisniewski,[63] M. Wittgen,[63] D. H. Wright,[63] H. W. Wulsin,[63] A. K. Yarritu,[63] C. C. Young,[63]
V. Ziegler,[63] X. R. Chen,[64] W. Park,[64] M. V. Purohit,[64] R. M. White,[64] J. R. Wilson,[64] A. Randle-Conde,[65]
S. J. Sekula,[65] M. Bellis,[66] P. R. Burchat,[66] T. S. Miyashita,[66] M. S. Alam,[67] J. A. Ernst,[67] N. Guttman,[68]
A. Soffer,[68] P. Lund,[69] S. M. Spanier,[69] R. Eckmann,[70] J. L. Ritchie,[70] A. M. Ruland,[70] C. J. Schilling,[70]
R. F. Schwitters,[70] B. C. Wray,[70] J. M. Izen,[71] X. C. Lou,[71] F. Bianchi[ab],[72] D. Gamba[ab],[72] M. Pelliccioni[ab],[72]
L. Lanceri[ab],[73] L. Vitale[ab],[73] N. Lopez-March,[74] F. Martinez-Vidal,[74] A. Oyanguren,[74] H. Ahmed,[75]
J. Albert,[75] Sw. Banerjee,[75] H. H. F. Choi,[75] K. Hamano,[75] G. J. King,[75] R. Kowalewski,[75] M. J. Lewczuk,[75]
C. Lindsay,[75] I. M. Nugent,[75] J. M. Roney,[75] R. J. Sobie,[75] T. J. Gershon,[76] P. F. Harrison,[76] T. E. Latham,[76]
E. M. T. Puccio,[76] H. R. Band,[77] S. Dasu,[77] Y. Pan,[77] R. Prepost,[77] C. O. Vuosalo,[77] and S. L. Wu[77]

(The *BABAR* Collaboration)

[1]*Laboratoire d'Annecy-le-Vieux de Physique des Particules (LAPP),
Université de Savoie, CNRS/IN2P3, F-74941 Annecy-Le-Vieux, France*
[2]*Universitat de Barcelona, Facultat de Fisica, Departament ECM, E-08028 Barcelona, Spain*
[3]*INFN Sezione di Bari[a]; Dipartimento di Fisica, Università di Bari[b], I-70126 Bari, Italy*
[4]*University of Bergen, Institute of Physics, N-5007 Bergen, Norway*
[5]*Lawrence Berkeley National Laboratory and University of California, Berkeley, California 94720, USA*
[6]*Ruhr Universität Bochum, Institut für Experimentalphysik 1, D-44780 Bochum, Germany*
[7]*University of British Columbia, Vancouver, British Columbia, Canada V6T 1Z1*
[8]*Brunel University, Uxbridge, Middlesex UB8 3PH, United Kingdom*
[9]*Budker Institute of Nuclear Physics, Novosibirsk 630090, Russia*
[10]*University of California at Irvine, Irvine, California 92697, USA*
[11]*University of California at Riverside, Riverside, California 92521, USA*
[12]*University of California at Santa Barbara, Santa Barbara, California 93106, USA*
[13]*University of California at Santa Cruz, Institute for Particle Physics, Santa Cruz, California 95064, USA*
[14]*California Institute of Technology, Pasadena, California 91125, USA*
[15]*University of Cincinnati, Cincinnati, Ohio 45221, USA*
[16]*University of Colorado, Boulder, Colorado 80309, USA*
[17]*Colorado State University, Fort Collins, Colorado 80523, USA*
[18]*Technische Universität Dortmund, Fakultät Physik, D-44221 Dortmund, Germany*
[19]*Technische Universität Dresden, Institut für Kern- und Teilchenphysik, D-01062 Dresden, Germany*
[20]*Laboratoire Leprince-Ringuet, CNRS/IN2P3, Ecole Polytechnique, F-91128 Palaiseau, France*
[21]*University of Edinburgh, Edinburgh EH9 3JZ, United Kingdom*
[22]*INFN Sezione di Ferrara[a]; Dipartimento di Fisica, Università di Ferrara[b], I-44100 Ferrara, Italy*
[23]*INFN Laboratori Nazionali di Frascati, I-00044 Frascati, Italy*
[24]*INFN Sezione di Genova[a]; Dipartimento di Fisica, Università di Genova[b], I-16146 Genova, Italy*
[25]*Indian Institute of Technology Guwahati, Guwahati, Assam, 781 039, India*
[26]*Harvard University, Cambridge, Massachusetts 02138, USA*
[27]*Harvey Mudd College, Claremont, California 91711*
[28]*Universität Heidelberg, Physikalisches Institut, Philosophenweg 12, D-69120 Heidelberg, Germany*
[29]*Humboldt-Universität zu Berlin, Institut für Physik, Newtonstr. 15, D-12489 Berlin, Germany*
[30]*Imperial College London, London, SW7 2AZ, United Kingdom*
[31]*University of Iowa, Iowa City, Iowa 52242, USA*
[32]*Iowa State University, Ames, Iowa 50011-3160, USA*
[33]*Johns Hopkins University, Baltimore, Maryland 21218, USA*
[34]*Laboratoire de l'Accélérateur Linéaire, IN2P3/CNRS et Université Paris-Sud 11,
Centre Scientifique d'Orsay, B. P. 34, F-91898 Orsay Cedex, France*
[35]*Lawrence Livermore National Laboratory, Livermore, California 94550, USA*
[36]*University of Liverpool, Liverpool L69 7ZE, United Kingdom*
[37]*Queen Mary, University of London, London, E1 4NS, United Kingdom*
[38]*University of London, Royal Holloway and Bedford New College, Egham, Surrey TW20 0EX, United Kingdom*
[39]*University of Louisville, Louisville, Kentucky 40292, USA*
[40]*Johannes Gutenberg-Universität Mainz, Institut für Kernphysik, D-55099 Mainz, Germany*
[41]*University of Manchester, Manchester M13 9PL, United Kingdom*
[42]*University of Maryland, College Park, Maryland 20742, USA*
[43]*University of Massachusetts, Amherst, Massachusetts 01003, USA*
[44]*Massachusetts Institute of Technology, Laboratory for Nuclear Science, Cambridge, Massachusetts 02139, USA*

[45]McGill University, Montréal, Québec, Canada H3A 2T8

[46]INFN Sezione di Milano[a]; Dipartimento di Fisica, Università di Milano[b], I-20133 Milano, Italy

[47]University of Mississippi, University, Mississippi 38677, USA

[48]Université de Montréal, Physique des Particules, Montréal, Québec, Canada H3C 3J7

[49]INFN Sezione di Napoli[a]; Dipartimento di Scienze Fisiche,
Università di Napoli Federico II[b], I-80126 Napoli, Italy

[50]NIKHEF, National Institute for Nuclear Physics and High Energy Physics, NL-1009 DB Amsterdam, The Netherlands

[51]University of Notre Dame, Notre Dame, Indiana 46556, USA

[52]Ohio State University, Columbus, Ohio 43210, USA

[53]University of Oregon, Eugene, Oregon 97403, USA

[54]INFN Sezione di Padova[a]; Dipartimento di Fisica, Università di Padova[b], I-35131 Padova, Italy

[55]Laboratoire de Physique Nucléaire et de Hautes Energies,
IN2P3/CNRS, Université Pierre et Marie Curie-Paris6,
Université Denis Diderot-Paris7, F-75252 Paris, France

[56]INFN Sezione di Perugia[a]; Dipartimento di Fisica, Università di Perugia[b], I-06100 Perugia, Italy

[57]INFN Sezione di Pisa[a]; Dipartimento di Fisica,
Università di Pisa[b]; Scuola Normale Superiore di Pisa[c], I-56127 Pisa, Italy

[58]Princeton University, Princeton, New Jersey 08544, USA

[59]INFN Sezione di Roma[a]; Dipartimento di Fisica,
Università di Roma La Sapienza[b], I-00185 Roma, Italy

[60]Universität Rostock, D-18051 Rostock, Germany

[61]Rutherford Appleton Laboratory, Chilton, Didcot, Oxon, OX11 0QX, United Kingdom

[62]CEA, Irfu, SPP, Centre de Saclay, F-91191 Gif-sur-Yvette, France

[63]SLAC National Accelerator Laboratory, Stanford, California 94309 USA

[64]University of South Carolina, Columbia, South Carolina 29208, USA

[65]Southern Methodist University, Dallas, Texas 75275, USA

[66]Stanford University, Stanford, California 94305-4060, USA

[67]State University of New York, Albany, New York 12222, USA

[68]Tel Aviv University, School of Physics and Astronomy, Tel Aviv, 69978, Israel

[69]University of Tennessee, Knoxville, Tennessee 37996, USA

[70]University of Texas at Austin, Austin, Texas 78712, USA

[71]University of Texas at Dallas, Richardson, Texas 75083, USA

[72]INFN Sezione di Torino[a]; Dipartimento di Fisica Sperimentale, Università di Torino[b], I-10125 Torino, Italy

[73]INFN Sezione di Trieste[a]; Dipartimento di Fisica, Università di Trieste[b], I-34127 Trieste, Italy

[74]IFIC, Universitat de Valencia-CSIC, E-46071 Valencia, Spain

[75]University of Victoria, Victoria, British Columbia, Canada V8W 3P6

[76]Department of Physics, University of Warwick, Coventry CV4 7AL, United Kingdom

[77]University of Wisconsin, Madison, Wisconsin 53706, USA

(Dated: February 23, 2011)

Using a sample of 122 million $\Upsilon(3S)$ events recorded with the *BABAR* detector at the PEP-II asymmetric-energy $e^+e^-$ collider at SLAC, we search for the $h_b(1P)$ spin-singlet partner of the $P$-wave $\chi_b(1P)$ states in the sequential decay $\Upsilon(3S) \to \pi^0 h_b(1P)$, $h_b(1P) \to \gamma \eta_b(1S)$. We observe an excess of events above background in the distribution of the recoil mass against the $\pi^0$ at mass $9902 \pm 4$(stat.) $\pm 1$(syst.) MeV/$c^2$. The width of the observed signal is consistent with experimental resolution, and its significance is 3.0 $\sigma$, including systematic uncertainties. We obtain the value $(3.7 \pm 1.1$ (stat.) $\pm 0.7$ (syst.) $) \times 10^{-4}$ for the product branching fraction $\mathcal{B}(\Upsilon(3S) \to \pi^0 h_b) \times \mathcal{B}(h_b \to \gamma \eta_b)$.

To understand the spin dependence of $q\bar{q}$ potentials for heavy quarks, it is essential to measure the hyperfine mass splitting for $P$-wave states. In the non-relativistic approximation, the hyperfine splitting is proportional to the square of the wave function at the origin, which is expected to be non-zero only for $L = 0$, where $L$ is the orbital angular momentum quantum number of the $q\bar{q}$ system. For $L = 1$, the splitting between the spin-singlet ($^1P_1$) and the spin-averaged triplet state ($\langle ^3P_J \rangle$) is expected to be $\Delta M_{\mathrm{HF}} = M(^3P_J) - M(^1P_1) \sim 0$. The $^1P_1$ state of bottomonium, the $h_b(1P)$, is the axial vec-

tor partner of the $P$-wave $\chi_{bJ}(1P)$ states. Its expected mass, computed as the spin-weighted center of gravity of the $\chi_{bJ}(1P)$ states [1], is $9899.87 \pm 0.27$ MeV/$c^2$. Higher-order corrections might cause a small deviation from this value, but a hyperfine splitting larger than 1 MeV/$c^2$ might be indicative of a vector component in the confinement potential [2]. The hyperfine splitting for the charmonium $^1P_1$ state $h_c$ is measured by the BES and CLEO experiments [3]–[5] to be $\sim 0.1$ MeV/$c^2$. An even smaller splitting is expected for the much heavier bottomonium system [2].

The $h_b(1P)$ state is expected to be produced in $\Upsilon(3S)$ decay via $\pi^0$ or di-pion emission, and to undergo a subsequent $E1$ transition to the $\eta_b(1S)$, with branching fraction (BF) $\mathcal{B}(h_b(1P) \to \gamma\eta_b(1S)) \sim (40-50)\%$ [2, 6]. The isospin-violating decay $\Upsilon(3S) \to \pi^0 h_b(1P)$ is expected to have a BF of about 0.1% [7, 8], while theoretical predictions for the transition $\Upsilon(3S) \to \pi^+\pi^- h_b(1P)$ range from $\sim 10^{-4}$ [7] up to $\sim 10^{-3}$ [9]. The CLEO experiment reported the 90% confidence level (C.L.) limit $\mathcal{B}(\Upsilon(3S) \to \pi^0 h_b(1P)) < 0.27\%$ [10] based on fewer than 0.5 million $\Upsilon(3S)$ events.

In this paper, we report evidence for the $h_b(1P)$ state in the decay $\Upsilon(3S) \to \pi^0 h_b(1P)$. The data sample used was collected with the BABAR detector [11] at the PEP-II asymmetric-energy $e^+e^-$ collider at the SLAC National Accelerator Laboratory and corresponds to 28 fb$^{-1}$ of integrated luminosity at a center-of-mass (CM) energy of 10.355 GeV, the mass of the $\Upsilon(3S)$ resonance. This sample contains $(122 \pm 1)$ million $\Upsilon(3S)$ events. Detailed Monte Carlo (MC) simulations [12] of samples of exclusive $\Upsilon(3S) \to \pi^0 h_b(1P)$, $h_b(1P) \to \gamma\eta_b(1S)$ decays (where the $h_b(1P)$ and $\eta_b(1S)$ are hereafter referred to as the $h_b$ and the $\eta_b$), and of inclusive $\Upsilon(3S)$ decays, are used in this study. These samples correspond to 34,000 signal and 215 million $\Upsilon(3S)$ events, respectively. In the inclusive $\Upsilon(3S)$ MC sample a BF of 0.1% is assumed for the decay $\Upsilon(3S) \to \pi^0 h_b$ [7].

The trajectories of charged particles are reconstructed using a combination of five layers of double-sided silicon strip detectors and a 40-layer drift chamber, both operating inside the 1.5-T magnetic field of a superconducting solenoid. Photons are detected, and their energies measured, with a CsI(Tl) electromagnetic calorimeter (EMC), also located inside the solenoid. The BABAR detector is described in detail elsewhere [11].

The signal for $\Upsilon(3S) \to \pi^0 h_b$ decays is extracted from a fit to the inclusive recoil mass distribution against the $\pi^0$ candidates $(m_{recoil}(\pi^0))$. It is expected to appear as a small excess centered near 9.9 GeV/$c^2$ on top of the very large non-peaking background produced from continuum events $(e^+e^- \to q\bar{q}$ with $q = u,d,s,c)$ and bottomonium decays. The recoil mass, $m_{recoil}(\pi^0) = \sqrt{(E^*_{beam} - E^*(\pi^0))^2 - p^*(\pi^0)^2}$ (where $E^*_{beam}$ corresponds to the sum of the beam particle CM energies), is computed in the $e^+e^-$ CM frame (denoted by the asterisk). We enhance the sensitivity of the search for the $h_b$ by exploiting the fact that the $h_b$ is expected to decay predominantly to $\gamma\eta_b$, and so require a reconstructed photon consistent with this decay. The precise measurement of the $\eta_b$ mass [13] defines a restricted energy range for a photon candidate compatible with this subsequent $h_b$ decay. A similar approach led to the observation by CLEO-c, and then by BES, of the $h_c$ in the decay chain $\psi(2S) \to h_c\pi^0 \to \eta_c\gamma\pi^0$ [3]–[5], where the $\eta_c$ was identified both exclusively (by reconstructing a large number of hadronic modes) and inclusively.

The photon from $h_b \to \gamma\eta_b$ decay is monochromatic in the $h_b$ rest-frame and is expected to peak at $\sim$490 MeV in the $e^+e^-$ CM frame, with a small Doppler broadening that arises from the motion of the $h_b$ in that frame; the corresponding energy resolution is expected to be $\sim 25$ MeV. The Doppler broadening is negligible compared with the energy resolution. Figure 1 shows the reconstructed CM energy distribution of such candidate photons in the region 250-1000 MeV for simulated $\Upsilon(3S) \to \pi^0 h_b$, $h_b \to \gamma\eta_b$ events before the application of selection criteria; the signal photon from $h_b \to \gamma\eta_b$ decay appears as a peak on top of a smooth background. We select monochromatic photon candidates with CM energy in the range 420-540 MeV (indicated by the shaded region in Fig. 1).
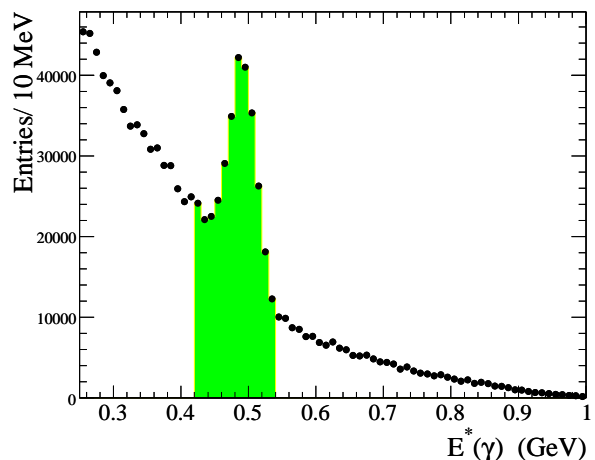


FIG. 1: The reconstructed CM energy distribution of the candidate photon $(\gamma)$ in simulated $\Upsilon(3S) \to \pi^0 h_b(1P)$, $h_b(1P) \to \gamma\eta_b(1S)$ events. The shaded region indicates the selected $E^*(\gamma)$ signal region.

We employ a simple set of selection criteria to suppress backgrounds while retaining a high signal efficiency. These selection criteria are chosen by optimizing the $S/\sqrt{B}$ ratio between the expected signal yield $(S)$ and the background $(B)$. The $\Upsilon(3S) \to \pi^0 h_b$, $h_b \to \gamma\eta_b$ MC signal sample is used in the optimization, while a small fraction (9%) of the total data sample is used to model the background. We estimate the contribution $B$ in the signal region, defined by $9.85 < m_{recoil}(\pi^0) < 9.95$ GeV/$c^2$, using the sidebands of the expected $h_b$ signal region, $9.80 < m_{recoil}(\pi^0) < 9.85$ GeV/$c^2$ and $9.95 < m_{recoil}(\pi^0) < 10.00$ GeV/$c^2$.

The decay of the $\eta_b$ is expected to result in high final-state track multiplicity. Therefore, we select a hadronic event candidate by requiring that it have four or more charged-particle tracks, and that the ratio of the second to zeroth Fox-Wolfram moments [14] be less than 0.6 [15].

For a given event, we require that a primary vertex

be found and fitted successfully from all charged-particle tracks in the event. We then constrain the candidate photons in that event to originate from that vertex.

A photon candidate is required to deposit a minimum laboratory energy of 50 MeV into a contiguous EMC crystal cluster that is isolated from all charged-particle tracks in that event. To ensure that the cluster shape is consistent with that for an electromagnetic shower, its lateral moment [16] is required to be less than 0.6.

A $\pi^0$ candidate is reconstructed as a photon pair with invariant mass $m(\gamma\gamma)$ in the range 55–200 MeV/$c^2$ (see Fig. 2). In the calculation of $m_{recoil}(\pi^0)$, the $\gamma$-pair invariant mass is constrained to the nominal $\pi^0$ value [1] in order to improve momentum resolution.

To suppress backgrounds due to misreconstructed $\pi^0$ candidates, we require $|\cos\theta_h| < 0.7$, where the helicity angle $\theta_h$ is defined as the angle between the direction of a $\gamma$ from a $\pi^0$ candidate in the $\pi^0$ rest-frame, and the $\pi^0$ direction in the laboratory.

Photons from $\pi^0$ decays are a primary source of background in the region of the monochromatic photon line from $h_b \to \gamma\eta_b$ transitions. A monochromatic photon candidate is rejected if, when combined with another photon in the event ($\gamma_2$), the resulting $\gamma\gamma_2$ invariant mass is within 15 MeV/$c^2$ of the nominal $\pi^0$ mass; this is called a $\pi^0$ veto. Similarly, a very large number of misreconstructed $\pi^0$ candidates results from the pairing of photons from different $\pi^0$'s. A $\pi^0$ candidate is rejected if either of its daughter photons satisfies the $\pi^0$ veto condition, with $\gamma_2$ not the other daughter photon. To maintain high signal efficiency, the $\pi^0$ veto condition is imposed only if the energy of $\gamma_2$ in the laboratory frame is greater than 200 MeV (150 MeV) for the monochromatic photon (for the $\pi^0$ daughters). With the application of these vetoes, and after all selection criteria have been imposed, the average $\pi^0$ candidate multiplicity per event is 2.17 for the full range of $m(\gamma\gamma)$, and 1.34 for the $\pi^0$ signal region ($110 < m(\gamma\gamma) < 150$ MeV/$c^2$). The average multiplicity for the monochromatic photon is 1.02; for 98.4% of $\pi^0$ candidates there is only one associated photon candidate.

To search for an $h_b$ signal, we select a $m_{recoil}(\pi^0)$ range from 9.73 to 10 GeV/$c^2$, and divide it into 90 intervals of 3 MeV/$c^2$ (see Fig. 3). For each $m_{recoil}(\pi^0)$ interval, the $m(\gamma\gamma)$ spectrum consists of a $\pi^0$ signal above combinatorial background (see Fig. 2). We obtain the $m_{recoil}(\pi^0)$ spectrum by extracting the $\pi^0$ signal yield in each interval of $m_{recoil}(\pi^0)$ from a fit to the $m(\gamma\gamma)$ distribution in that interval. The $m_{recoil}(\pi^0)$ distribution is thus obtained as the fitted $\pi^0$ yield and its uncertainty for each interval of $m_{recoil}(\pi^0)$.

We use the MC background and $\pi^0$-signal distributions directly in fitting the data [17]. For each $m_{recoil}(\pi^0)$ interval in MC, we obtain histograms in 0.1 MeV/$c^2$ intervals of $m(\gamma\gamma)$ corresponding to the $\pi^0$-signal and background distributions. The $\pi^0$-signal distribution is obtained by requiring matching of the reconstructed to
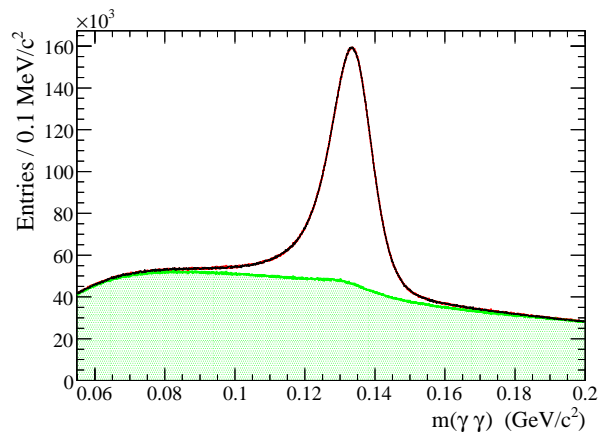


FIG. 2: The result of the fit to the $m(\gamma\gamma)$ distribution in data (data points) for the full range of $m_{recoil}(\pi^0)$. The solid histogram shows the fit result, and is essentially indistinguishable from the data; the shaded histogram corresponds to the background distribution.

the generated $\pi^0$'s on an candidate-by-candidate basis (termed "truth-matching" in the following discussion). The histogram representing background is obtained by subtraction of the $\pi^0$-signal from the total distribution.

For both signal and background data the qualitative changes in shape over the full range of $m_{recoil}(\pi^0)$ are quite well reproduced by the MC. However, the $\pi^0$ signal distribution from data is slightly broader, and the peak mass value slightly higher, than for the simulation. The $m(\gamma\gamma)$ background shape also differs between data and MC. To address these differences, the MC $\pi^0$ signal is displaced in mass and smeared by a double Gaussian function with different mean and width values; the MC background distribution is weighted according to a polynomial in $m(\gamma\gamma)$. The signal-shape and background weighting-parameter values are obtained from a fit to the $m(\gamma\gamma)$ distribution in data for the full range of $m_{recoil}(\pi^0)$. At each step in the fitting procedure, the $\pi^0$-signal and background distributions are normalized to unit area, and a $\chi^2$ between a linear combination of these MC histograms and the $m(\gamma\gamma)$ distribution in data is computed. The result, shown in Fig. 2, indicates that the fit function provides an adequate description of the data ($\chi^2/NDF=1446/1433$; $NDF$=Number of Degrees of Freedom). The background distribution exhibits a small peak at the $\pi^0$ mass, due to interactions in the detector material of the type $n\pi^+ \to p\pi^0$ or $p\pi^- \to n\pi^0$ that cannot be truth-matched. The normalization of this background to the non-peaking background is obtained from the MC simulation, which incorporates the results of detailed studies of interactions in the detector material performed using data [18]. This peak is displaced and smeared in the same way as the primary $\pi^0$ signal.

The fits to the individual $m(\gamma\gamma)$ distributions are per-

formed with the smearing and weighting parameters fixed to the values obtained from the fit shown in Fig. 2. In this process, the MC signal and background distributions for each $m_{recoil}(\pi^0)$ interval are shifted, smeared, and weighted using the fixed parameter values, and then normalized to unit area. Thus, only the signal and background normalizations are free parameters in each fit. The $\chi^2$-fit to the data then gives the value and uncertainty of the coefficient multiplying the $\pi^0$-signal histogram as the number of $\pi^0$ events and its uncertainty. The fits to the 90 $m(\gamma\gamma)$ distributions provide good descriptions of the data, with an average $\langle \chi^2/NDF \rangle = 0.98 \pm 0.03$ ($NDF$=1448), where the value $\pm 0.03$ is the r.m.s. of the distribution. We verify that the fitted $\pi^0$ yield is consistent with the number of truth-associated $\pi^0$'s in MC to ensure that the $\pi^0$ selection efficiency is well-determined using truth-matching, and to check the validity of the $\pi^0$-signal extraction procedure.

Figure 3 shows the $m_{recoil}(\pi^0)$ distribution obtained in data by applying the $\pi^0$-signal extraction procedure. To search for an $h_b$ signal, we perform a binned $\chi^2$ fit to this spectrum using a fit function that contains signal and background contributions. The signal component is parametrized with the sum of two Crystal Ball [19] functions with parameter values determined from signal $\Upsilon(3S) \rightarrow \pi^0 h_b$ MC events. The background function is obtained from the background distribution of an inclusive MC sample that is weighted to accurately model the distribution in data. The weighting function is a fifth order polynomial with parameters set from a fit of the ratio of the $m_{recoil}(\pi^0)$ distributions in data and MC excluding the $h_b$ signal region (9.87–9.93 GeV/$c^2$). We obtain a corrected MC background distribution by applying this weight over the full range of $m_{recoil}(\pi^0)$.

We fit the corrected MC background distribution with a sixth order polynomial function. To improve sensitivity, the background function is fixed in the fit to data. All the parameters of the $h_b$ signal lineshape except the peak position and yield are fixed. The number of $h_b$ events obtained from the fit is $9145 \pm 2804$, and the $h_b$ fitted mass value is $m = 9902 \pm 4$ MeV/$c^2$. The distribution of the normalized residuals is described by a Gaussian function with mean and width values consistent with zero and one, respectively; this confirms that the uncertainties associated with the individual $\pi^0$ signals are reliable.

In order to determine the statistical significance of the signal we repeat the fit with the $h_b$ mass fixed to the center of gravity of the $\chi_{bJ}(1P)$ states, $m = 9900$ MeV/$c^2$. The signal yield obtained from this fit is $8959 \pm 2796$. The statistical significance of the signal is calculated from the square-root of the difference in $\chi^2$ for this fit with and without a signal component; this gives a value of 3.2 standard deviations. Figure 4 represents the results of a scan performed as a function of the assumed $h_b$ mass. Each point in this figure corresponds to the fitted signal yield with the $h_b$ mass parameter fixed.
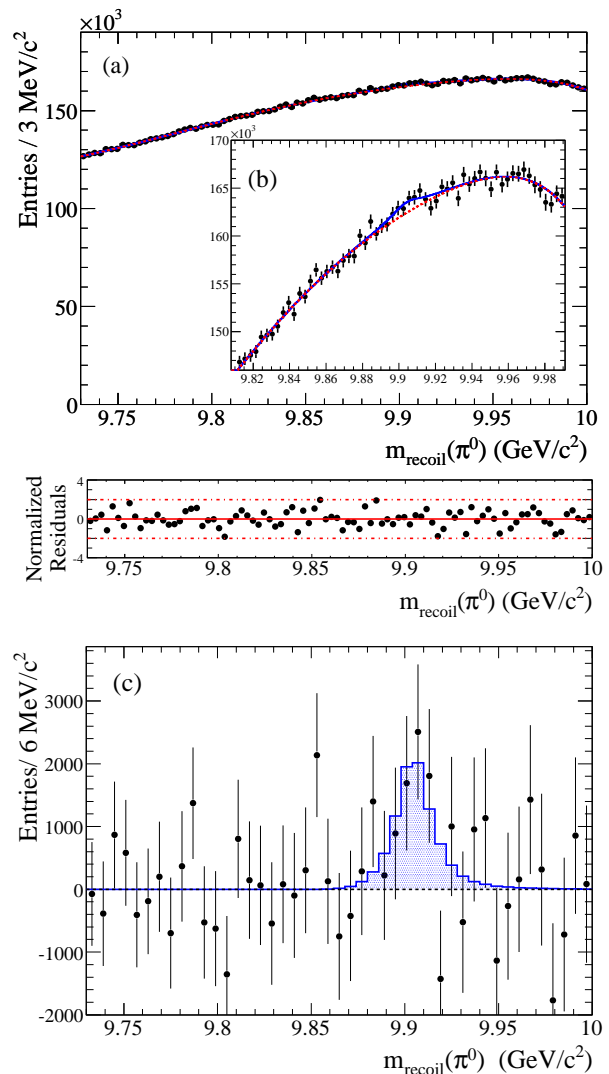


FIG. 3: (a) The $m_{recoil}(\pi^0)$ distribution in the region $9.73 < m_{recoil}(\pi^0) < 10$ GeV/$c^2$ for data (points); the solid curve represents the fit function described in the text. The normalized residuals are shown underneath. (b) (inset) Expanded view of the signal region; the dashed curve represents the background function. (c) The $m_{recoil}(\pi^0)$ spectrum after subtracting background; the shaded histogram represents the signal function resulting from the fit to the data.

We obtain an estimate of systematic uncertainty on the number of $\pi^0$'s in each $m_{recoil}(\pi^0)$ interval by repeating the fits to the individual $m(\gamma\gamma)$ spectra with the lineshape parameters corresponding to Fig. 2 varied within their uncertainties. The distribution of the net uncertainty varies as a third order polynomial in $m_{recoil}(\pi^0)$. We estimate a systematic uncertainty of $\pm 210$ events on the $h_b$ signal yield due to the $\pi^0$-yield extraction procedure by evaluating this function at the fitted $h_b$ mass value.

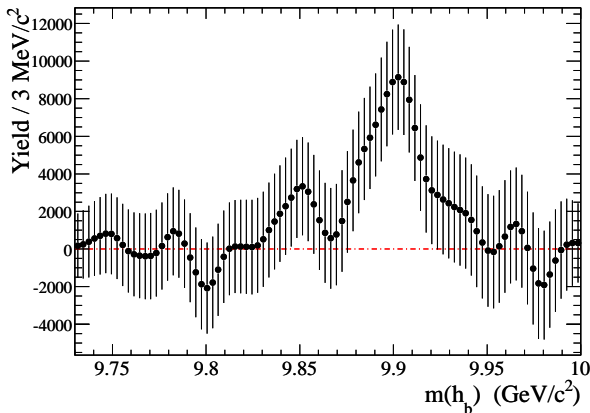The dominant systematic uncertainty on the measured

FIG. 4: The fitted yields as a function of the assumed $h_b$ mass.

$h_b$ yield is due to the choice of the shape of the $m_{recoil}(\pi^0)$ background distribution. It is estimated from an ensemble of background function parameters, obtained by perturbing the nominal fit values by random amounts sampled from the covariance matrix, with correlations taken into account. A sample of 1500 sets of randomized parameter values is obtained by this procedure. For each such set, we fit the data distribution with the background function fixed to the parameter values of the set. The distribution of the signal yields is found to be Gaussian with mean coinciding with the nominal fit value and $\sigma = 1059$ events. Similarly, we obtain a systematic uncertainty of $\pm 0.5$ MeV/$c^2$ on the $h_b$ mass.

The systematic uncertainty associated with the choice of signal lineshape is estimated by varying the signal function parameters, which were fixed in the fit, by $\pm 1\,\sigma$. Systematic uncertainties of $\pm 75$ events and $\pm 0.5$ MeV/$c^2$ are obtained for the $h_b$ yield and mass, respectively.

After combining these systematic uncertainty estimates in quadrature, we obtain an effective signal significance of 3.0 standard deviations. We find an $h_b$ yield of $9145 \pm 2804 \pm 1082$ events and an $h_b$ mass value $m = 9902 \pm 4 \pm 1$ MeV/$c^2$, where the first error is statistical and the second systematic. The resulting hyperfine splitting with respect to the center of gravity of the $\chi_{bJ}(1P)$ states is thus $\Delta_{\mathrm{HF}} = +2 \pm 4 \pm 1$ MeV/$c^2$, which agrees within error with model predictions [7, 8].

To convert the yield into a measurement of the product BF for the sequential decay $\Upsilon(3S) \to \pi^0 h_b$, $h_b \to \gamma \eta_b$, we determine the efficiency $\epsilon_S$ from MC, requiring that the signal $\pi^0$ and the $\gamma$ be truth-matched. The resulting efficiency is $\epsilon_S = 15.8 \pm 0.2\%$. MC studies indicate that photons that are not from an $h_b \to \gamma \eta_b$ transition can satisfy the selection criteria when only the $\Upsilon(3S) \to \pi^0 h_b$ transition is truth-matched. This causes a fictitious increase in the $h_b$ signal efficiency to $\epsilon = 17.9 \pm 0.2\%$. Therefore, the efficiency for observed $h_b$ signal events that do not

correspond to $h_b \to \gamma \eta_b$ decay is $\Delta\epsilon = 2.1\%$. However, there is no current experimental information on the production of such non-signal photons in $h_b$ and $\eta_b$ decays. Furthermore, the above estimate of efficiencies in MC does not account for photons from hadronic $h_b$ decays, since the signal MC requires $h_b \to \gamma \eta_b$. We thus assume that random photons from hadronic $h_b$ decays have the same probability $\Delta\epsilon$ to satisfy the monochromatic photon selection criteria as those from $\eta_b$ decays. We assume a 100% uncertainty on the value of $\Delta\epsilon$ when estimating the systematic error on the product BF.

We estimate the product BF for $\Upsilon(3S) \to \pi^0 h_b$, $h_b \to \gamma \eta_b$ by dividing the fitted signal yield $N$, corrected for the estimated total reconstruction efficiency, by the number of $\Upsilon(3S)$ events $N_{\Upsilon(3S)}$ in the data sample. We obtain the following expression for the product BF:

$$\mathcal{B}(\Upsilon(3S) \to \pi^0 h_b) \times \mathcal{B}(h_b \to \gamma \eta_b) = \frac{N/(N_{\Upsilon(3S)}\,\epsilon_S)}{C}, \quad (1)$$

where

$$C = 1 + \frac{\Delta\epsilon/\epsilon_S}{\mathcal{B}(h_b \to \gamma \eta_b)} \quad (2)$$

is the correction factor to the efficiency $\epsilon_S$ to account for the non-signal hadronic $h_b$ and $\eta_b$ contributions. In this equation, we assume a BF value $\mathcal{B}(h_b \to \gamma \eta_b) = 45 \pm 5\%$ according to the current range of theory predictions. The corresponding correction factor is $1 - C \sim 30\%$, with a systematic uncertainty dominated by the uncertainty on $\Delta\epsilon$.

We obtain $\mathcal{B}(\Upsilon(3S) \to \pi^0 h_b) \times \mathcal{B}(h_b \to \gamma \eta_b) = (3.7 \pm 1.1 \pm 0.7) \times 10^{-4}$, where the first uncertainty is statistical and the second systematic. The result is consistent with the prediction of Ref. [8], which estimates $4 \times 10^{-4}$ for the product BF. Since the $h_b$-decay uncertainty reduces the significance of the product BF relative to that of the $h_b$ production, we may interpret the former result as an upper limit. From an ensemble of simulated events using the measured product BF value, and the statistical and associated systematic uncertainties (assumed to be Gaussian) as input, we obtain $\mathcal{B}(\Upsilon(3S) \to \pi^0 h_b) \times \mathcal{B}(h_b \to \gamma \eta_b) < 5.8 \times 10^{-4}$ at 90% C.L.

In summary, we have found evidence for the decay $\Upsilon(3S) \to \pi^0 h_b$, with a significance of 3.0 standard deviations, including systematic uncertainties. The measured mass value, $m = 9902 \pm 4(\mathrm{stat.}) \pm 1(\mathrm{syst.})$ MeV/$c^2$, is consistent with the expectation for the $h_b(1P)$ bottomonium state, the axial vector partner of the $\chi_{bJ}(1P)$ triplet of states. We obtain $\mathcal{B}(\Upsilon(3S) \to \pi^0 h_b) \times \mathcal{B}(h_b \to \gamma \eta_b) = (3.7 \pm 1.1\ (\mathrm{stat.})\ \pm 0.7\ (\mathrm{syst.})\ ) \times 10^{-4}\ (< 5.8 \times 10^{-4}$ at 90% C.L.).

---

[∗] Now at Temple University, Philadelphia, Pennsylvania 19122, USA

[†] Also with Università di Perugia, Dipartimento di Fisica, Perugia, Italy

[‡] Now at University of South Alabama, Mobile, Alabama 36688, USA

[§] Also with Università di Sassari, Sassari, Italy

[1] K. Nakamura *et al.* (Particle Data Group), Journal of Physics G **37**, 075021 (2010).

[2] S. Godfrey and J.L. Rosner, Phys. Rev. D **66**, 014012 (2002).

[3] M. Ablikim *et al.* (BES Collaboration), Phys. Rev. Lett. **104**, 132002 (2010).

[4] J.L. Rosner *et al.* (CLEO Collaboration), Phys. Rev. Lett. **95**, 102003 (2005); S. Dobbs *et al.* (CLEO Collaboration), Phys. Rev. Lett. **101**, 182003 (2008).

[5] G.S. Adams *et al.* (CLEO Collaboration), Phys. Rev. D **80**, 051106 (2009).

[6] J.L. Rosner *et al.* (CLEO Collaboration), Phys. Rev. Lett. **95**, 102003 (2005).

[7] M.B. Voloshin, Sov. J. Nucl. Phys. **43**, 1011 (1986).

[8] S. Godfrey, J. Phys. Conf. Ser. **9**, 123 (2005).

[9] Y.P. Kuang and T.M. Yan, Phys. Rev. D **24**, 2874 (1981); Y.P. Kuang, S.F. Tuan, and T.M. Yan, Phys. Rev. D **37**, 1210 (1988); Y.P. Kuang and T.M. Yan, Phys. Rev. D **41**, 155 (1990); S.F. Tuan, Mod. Phys. Lett. **A7**, 3527 (1992).

[10] F. Butler *et al.* (CLEO Collaboration), Phys. Rev. D **49**, 40 (1994).

[11] B. Aubert *et al.* (*BABAR* Collaboration), Nucl. Instrum. Meth. **A479**, 1 (2002).

[12] The MC events are generated using the Jetset7.4 and PYTHIA programs to describe the hadronization process from the Lund string fragmentation model with final-state radiation included. [18].

[13] B. Aubert *et al.* (*BABAR* Collaboration), Phys. Rev. Lett. **101**, 071801 (2008); [Erratum-ibid. **102**, 029901 (2009)].

[14] G.C. Fox and S. Wolfram, Nucl. Phys. **B149**, 413 (1979).

[15] This quantity is indicative of the collimation of an event topology, with values close to one for jetlike events; the kinematics of a heavy object such as the $\eta_b$ decaying hadronically result in a more spherical event.

[16] A. Drescher *et al.*, Nucl. Instrum. Meth. **237**, 464 (1985).

[17] In MC simulations, fits to the individual $m(\gamma\gamma)$ spectra that make use of a polynomial background function and various combinations of Crystal Ball [19] and/or Gaussian signal functions proved unsatisfactory at the high statistical precision necessary.

[18] S. Agostinelli *et al.* (GEANT4 Collaboration), Nucl. Instrum. Meth. **506**, 250 (2003); T. Sjöstrand and M. Bengtsson, Computer Physics Commun. **43** (1987) 367.

[19] M.J. Oreglia, Ph.D Thesis, SLAC-R-**236** (1980); J.E. Gaiser, Ph.D Thesis, SLAC-R-**255** (1982); T. Skwarnicki, Ph.D Thesis, DESY F31-86-02 (1986).